Astrophysical Masers and their Environments
Proceedings IAU Symposium No. 242, 2007
J.M. Chapman, & W.A. Baan, eds.

doi:10.1017/S1743921307013014

A 20-year H_2O maser monitoring program with the Medicina 32-m telescope

J. Brand[1], M. Felli[2], R. Cesaroni[2], C. Codella[3], G. Comoretto[2], S. Di Franco[4], F. Massi[2], L. Moscadelli[2], R. Nesti[2], L. Olmi[3], F. Palagi[3], F. Palla[2], D. Panella[2], and R. Valdettaro[2]

[1]INAF-Istituto di Radioastronomia, Bologna, Italy
email: brand@ira.inaf.it

[2]INAF-Osservatorio Astrofisico di Arcetri, Florence, Italy

[3]INAF-Istituto di Radioastronomia, Sez. di Firenze, Florence, Italy

[4]Dip. di Astronomia, Università degli Studi di Firenze, Florence, Italy

Abstract. The Arcetri/Bologna H_2O maser group has been monitoring the 1.3-cm water maser emission from a sample of 43 star-forming regions (SFRs) and 22 late-type stars for about 20 years at a sampling rate of 4-5 observations each year, using the 32-m Medicina Radio Telescope (HPBW 1.′9 at 22 GHz). For the late-type stars we observe representative samples of OH/IR-stars, Mira's, semi-regular variables, and supergiants. The SFR-sample spans a large interval in FIR luminosity of the associated Young Stellar Object (YSO), from 20 $L_\odot$ to 1.5 $\times 10^6$ $L_\odot$, and offers a unique data base for the study of the long-term (years) variability of the maser emission in regions of star formation.

This presentation concerns only the masers in SFRs. The information obtained from single-dish monitoring is complementary to what is extracted from higher-resolution (VLA and VLBI) observations, and can better explore the velocity domain and the long-term variability therein.

We characterize the variability of the sources in various ways and we study how it depends on the luminosity and other properties of the associated YSO and its environment.

Keywords. masers, astronomical data bases: miscellaneous

1. Introduction

Twenty years ago in 1987, in the same month that this Symposium is held, we registered the first spectrum of many in our H_2O maser monitoring campaign. Since then, four or five times a year we have taken a spectrum of 43 masers in star-forming regions and in 22 circumstellar envelopes of late-type stars. The latter will not be discussed here - instead we refer to the poster by Engels, Winnberg, Brand, & Jimenez-Esteban in these proceedings.

After the presentation and analysis of a sub-set of our database of masers in SFRs (Valdettaro *et al.* 2002; Brand *et al.* 2003; Brand *et al.* 2005) we are now preparing to release our entire archive.

Interstellar water masers are highly variable, regarding both the velocities at which emission is detected and the intensity of that emission. The importance of the maser monitoring database lies above all in the opportunity it offers to study the *long-term variability*, i.e. on a scale of years. Valdettaro *et al.* (2002) presented a number of tools with which to visualize and quantify the maser data. One of the visual tools is the velocity-time-flux density diagram (hereafter: VtF-diagram), which allows a bird's eye view of the behaviour of the emission during the monitoring period (cf. Fig. 3). In view of the complex patterns

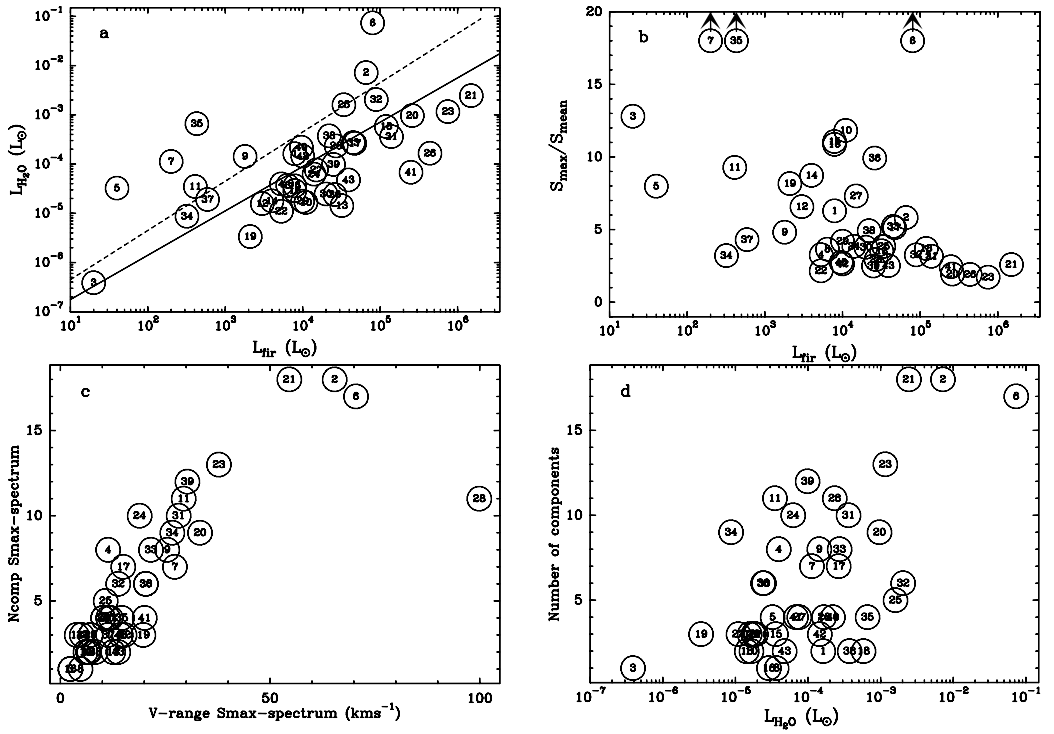

Figure 1. a. The luminosity of the maser, derived from the spectrum with the maximum integrated flux density during the monitoring, as a function of $L_{\rm fir}$. The drawn line is a bisector least-squares fit to the data. The dashed line indicates the relation between the two luminosities found by Wouterloot *et al.* (1995). **b.** Variability index $S_{\rm max}/S_{\rm mean}$ versus $L_{\rm fir}$.. Three objects that have values outside the range shown are indicated by the symbols with the arrows. The deviation of nr. 6 (KLIRc2) is caused by a particularly strong burst (cf. Fig. 2b). **c.** The number of emission components ($> 5\sigma$) versus the range in velocity they cover, for the spectra with maximum integrated flux density of each source. **d.** As c, but showing the number of components as a function of the H_2O luminosity derived from those spectra.

that emerge from these diagrams which we derive for each source, the simple standard analysis of the variation of the integrated intensity, although still indicative of the overall maser emission, is clearly limited and may miss more physically interesting aspects of the activity within star-forming regions. For example: a) velocity drifts, either steady and continuous over the entire monitoring period or occasional, preferentially after bursts; b) bursts occuring at different velocities and their frequency of occurrence; c) correlated or anti-correlated intensity variations at different velocities, d) the fraction of time in which the maser is active, either in an absolute sense or in each individual velocity channel. Below we highlight these and other aspects, to illustrate how the database can be mined to yield useful physical information.

2. Results

2.1. *General properties*

The general properties of the maser emission, especially as a function of the luminosity $L_{\rm fir}$ of the associated IRAS (pumping) source, were extensively analyzed by Brand *et al.* (2003). Here we present four of the figures from that paper, updated for the whole sample. The properties and trends found for the sub-sample are confirmed: there is a correlation

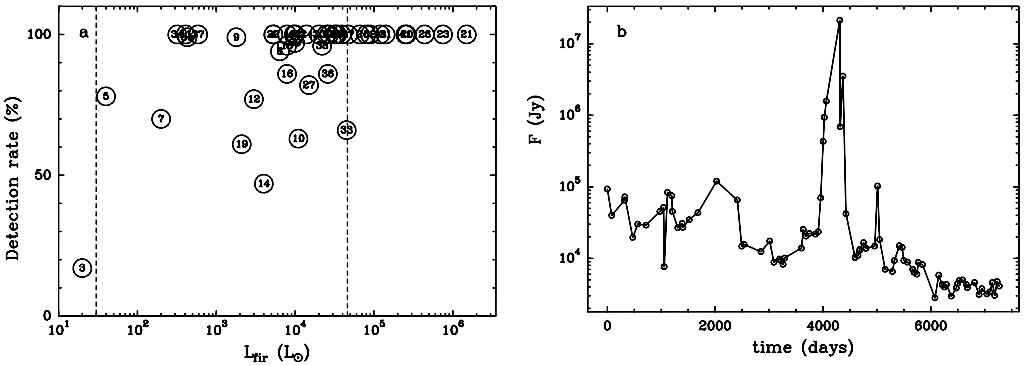

Figure 2. a. Detection rate (at levels $> 5\sigma$) of masers as function of $L_{\rm fir}$. The dashed lines separate $L_{\rm fir}$-ranges with different maser detection rates (see text). **b.** Monster-burst in KLIRc2 (1997-1999): flux density versus time.

between the maximum maser luminosity and $L_{\rm fir}$ [$\log L_{\rm H_2O} = (-7.66 \pm 0.47) - (0.90 \pm 0.12)\log L_{\rm fir}$], in good agreement with the upper limit found from single-epoch observations of many maser sources (Fig. 1a; cf. Wouterloot *et al.* 1995). The ratio between the maximum and the mean integrated flux density can be used as a variability index; its decrease with increasing $L_{\rm fir}$ (Fig. 1b) shows that more luminous sources are associated with more stable masers. The correlations found between the number of emission components and their velocity range (Fig. 1c) and the maser luminosity (Fig. 1d) indicate that higher maser power goes into more emission channels, spread over a larger range in velocity. Figure 2a shows the detection rate ($> 5\sigma$) of maser emission as a function of $L_{\rm fir}$. For masers associated with low-luminosity pumps ($L_{\rm fir} < 30$ $L_\odot$) the maser is undetected much of the time (det. rate 17%). Although there is only one object in this range, this luminosity limit is consistent with the 25 $L_\odot$ found by Claussen *et al.* (1996). For 30 $L_\odot < L_{\rm fir} < 4.6 \times 10^4$ $L_\odot$, the average detection rate is 90%, with a dispersion of 15%. This can be understood if for an individual source the masing conditions depend on the orientation of the outflow(s) and on the presence of high-density molecular gas rather than on $L_{\rm fir}$; only for $L_{\rm fir} > 4.6 \times 10^4$ $L_\odot$, the exciting source is the dominant factor and the maser is always detected.

2.2. *Bursts and velocity drifts*

Bursts of maser emission can easily be spotted in the VtF-diagram, and appear to be quite common. Often they also stand out in the maser light curve, as shown in Fig. 2b for KLIRc2. This burst began on Dec. 14, 1997 and reached a maximum flux density of 2.1×10^7 $L_\odot$ (an increase by a factor of almost 1300) after 400 days. After another 284 days the source was back to its normal level. Note that the general trend over the years is for the flux density to *decrease*. Figure 3 shows four examples of VtF-diagrams in which we have indicated possible velocity gradients of maser components. The indicated drifts (both acceleration and decelaration) are of the order of $0.3-3.5$ km s^{-1} yr^{-1}. In the case of IRAS20126+4104 , component (2) (Fig. 3b) the reality of the indicated drift could be verified by means of multi-epoch high spatial resolution observations (see Moscadelli *et al.* 2005): from 3-epoch VLBI observations absolute positions and proper motions of various maser spots could be determined. Extrapolating the proper motions backwards and forwards in time showed the spots' positions to be in good agreement with those actually measured in observations with VLBA (earlier) and MERLIN (later). Moscadelli *et al.* (2005) interpreted these observations in terms of maser spots being located on the walls of a conical outflow originating at the YSO where a stellar jet impacts with the

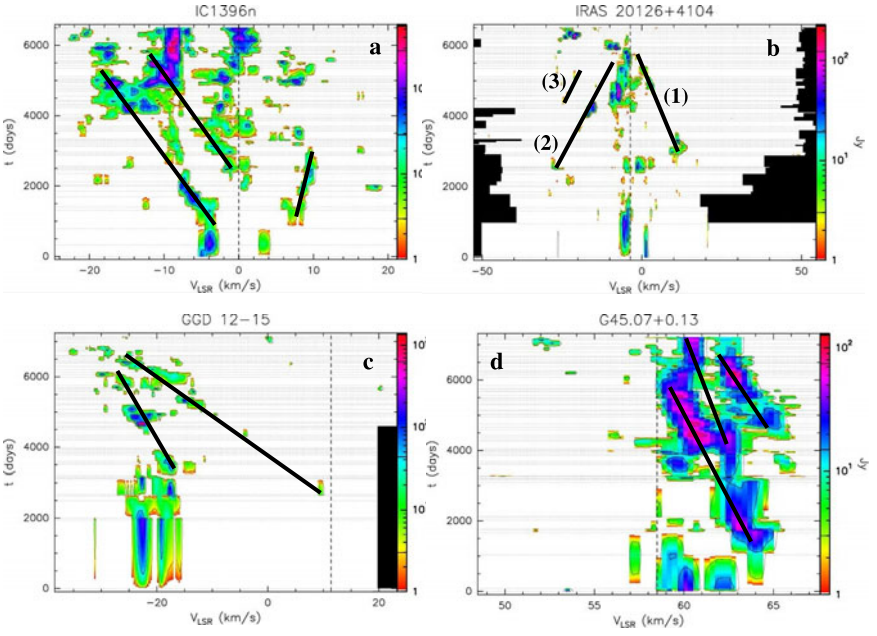

Figure 3. Velocity gradients in VtF-diagrams. Drawn lines indicate possible velocity drifts of maser components. **a.** IC1396N **b.** IRAS20126+4104 **c.** GGD12–15 **d.** G45.07+0.13. (See the online version for colour contours).

surrounding material. Subsequent deceleration leads to the temporal behaviour of the maser features as seen in the single-dish observations of Fig. 3b. We note, by the way, that a look at Fig. 3 already makes it evident that an instantaneous maser spectrum of a source will usually not be a "typical" representation of the maser emission of that source; in fact, a "typical" maser spectrum is unlikely to exist.

2.3. *Super-variability*

Apart from variations on relatively short timescales, longer-period "super-variability" has been found as well. Several examples are shown in Fig. 4, where the total maser output is shown as a function of time. This phenomenon, with periods between 4 and >16 years, is only brought to light in monitoring programs like this - in fact it has also been found in the Pushchino monitoring data (e.g., Lekht *et al.* 2001; Lekht *et al.* 2002). It may be caused by periodic variations in the wind of the Young Stellar Object.

3. Future Work

The 20-year database is presented in Felli *et al.* (2007); plots of all spectra and all derived information (VtF-diagrams, upper envelopes, light curves etc.) will be available on-line (http://www.arcetri.astro.it/science/Radio). This will be followed by a general analysis of the database, and by studies of individual objects. We think that a detailed knowledge of the immediate surroundings of the YSOs is essential in understanding the variability of the masers. This is illustrated for instance by the predominantly blue

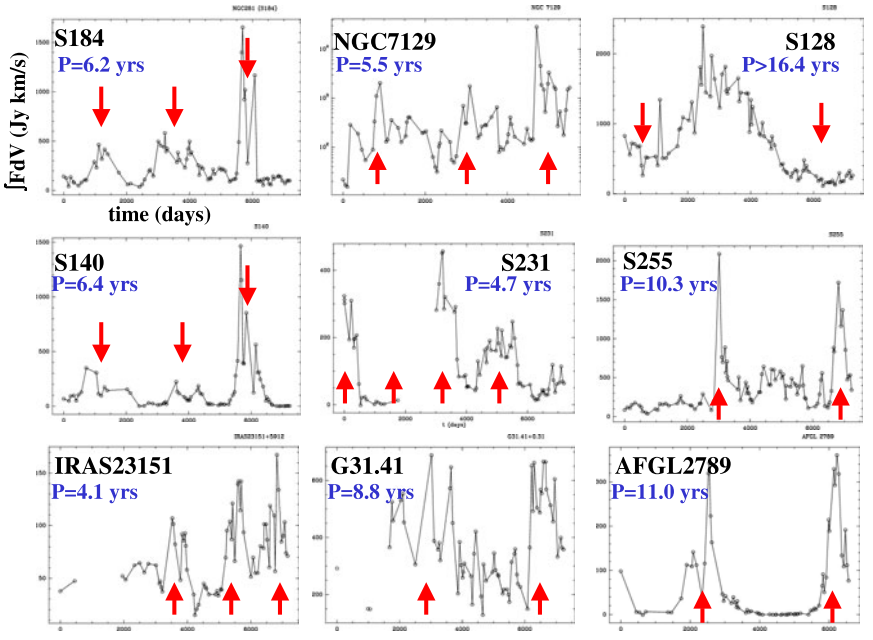

Figure 4. Long-term ("super") variability in maser sources. We show maser lightcurves ($\int FdV$ versus time) for nine objects. Approximate periods are indicated in each panel. The arrows indicate the location of the maxima (minima, for S128) from which the periods were derived.

tails sometimes seen in the detection rate histograms (see Brand *et al.* 2003), which we interpret as indicating a fortuitous alignment along the line-of-sight to the YSO of a highly collimated outflow, allowing one to see the amplification of the radio continuum emission of a compact HII region surrounding that YSO. Therefore we shall continue the monitoring, and carry out follow-up observations with interferometers.

References

Brand, J., Cesaroni, R., Comoretto, G., Felli, M., Palagi, F., Palla, F., & Valdettaro, R. 2003, *A&A* 407, 573

Brand, J., Cesaroni, R., Comoretto, G., Felli, M., Palagi, F., Palla, F., & Valdettaro, R. 2005, *Ap&Sp. Sci* 295, 133

Claussen, M. J., Wilking, B. A., Benson, P. J., *et al.* 1996, *ApJS*, 106, 111

Felli, M., Brand, J., Cesaroni, R., *et al.* 2007, *A&A*, *in preparation*

Lekht, E. E, Mendoza-Torres, J. E., & Berulis, I. I. 2002, *Astron. Rep.* 46, 57

Lekht, E. E, Paschenko, M. I., & Berulis, I. I. 2001, *Astron. Rep.* 45, 949

Moscadelli, L., Cesaroni, R., & Rioja M. J. 2005, *A&A* 438, 889

Valdettaro, R., Palla, F., Brand, J., Cesaroni, R., Comoretto, G., Felli, M., & Palagi, F. 2002, *A&A* 383, 244

Wouterloot, J. G. A, Fiegle K., Brand, J., & Winnewisser, G. 1995, *A&A* 301, 236 (Erratum: 1997, A&A 319, 360)